2017-08-10

Transcription of the Virus-like Agent Responsible for Carcinogenesis in Bicolor Damselfish

Jazmine Pritchett
University of Miami, jazziebelles@gmail.com

UNIVERSITY OF MIAMI

TRANSCRIPTION OF THE VIRUS-LIKE AGENT RESPONSIBLE FOR CARCINOGENESIS IN BICOLOR DAMSELFISH

By

Jazmine S. Pritchett

A THESIS

Submitted to the Faculty
of the University of Miami
in partial fulfillment of the requirements for
the degree of Master of Science

Coral Gables, Florida

August 2017

UNIVERSITY OF MIAMI

A thesis submitted in partial fulfillment of
the requirements for the degree of
Master of Science

TRANSCRIPTION OF THE VIRUS-LIKE AGENT RESPONSIBLE FOR CARCINOGENESIS IN BICOLOR DAMSELFISH

Jazmine S. Pritchett

Approved:

_____ Michael Schmale, Ph.D. Professor of Marine Biology And Ecology	_____ Marjorie Oleksiak, Ph.D. Associate Professor of Marine Biology and Ecology
_____ Nevis L. Fregien, Ph.D. Associate Professor of Cell Biology	_____ Guillermo Prado, Ph.D. Dean of the Graduate School

PRITCHETT, JAZMINE S. (M.S., Marine Biology and Fisheries)

(August 2017)

Transcription of the Virus-like Agent Responsible for Carcinogenesis in Bicolor Damselfish.

Abstract of a thesis at the University of Miami.

Thesis supervised by Professor Michael Schmale.
No. of pages in text. (42)

Damselfish Neurofibromatosis (DNF) is a naturally occurring cancer that affects Bicolor Damselfish (*Stegastes partitus*) located on South Florida reefs. Damselfish Neurofibromatosis is characterized by tumor development within the pigmented cells of the skin (chromatophoromas) as well as Schwann cells (neurofibromas and malignant peripheral nerve sheath tumors). Damselfish Neurofibromatosis has been shown to be caused by a virus-like agent with a 2.4 kb DNA genome named the Damselfish Virus-like Agent (DVLA). Studies of DVLA have shown that this DNA is located and replicates within the mitochondria of infected cells. Five RNAs are transcribed from the DVLA genome but the mechanism of how the genome is transcribed remains unknown. The purpose of this study was to further investigate how the DNA genome of DVLA is transcribed within the cells and how this ultimately affects the tumorigenesis of the virus-like agent. Primer sets were designed which recognize all five transcripts (DVLA stem) or only the longest transcript (DVLA loop) of DVLA. Inhibition of RNA polymerase II with triptolide caused significantly more inhibition of nuclear transcripts than of DVLA stem and the mitochondrial transcripts. However, DVLA loop showed no significant difference in inhibition from either the nuclear or mitochondrial transcripts. Treatment

with ethidium bromide to block mitochondrial RNA transcription caused significantly greater inhibition of the DVLA and mitochondrial transcripts compared to the nuclear transcripts. These results are consistent with the transcription of DVLA RNAs by mitochondrial rather than nuclear polymerases. DVLA loop had a strong positive correlation with cytochrome-b and D-loop in total RNA levels. DVLA loop had a short half-life, high synthesis rate, and low copy number count similar to D-loop. These similarities suggest that DVLA loop may serve a similar role as D-loop in RNA transcription and the initiation of DNA replication. Transcripts identified with DVLA stem primers had the longest half-life of the transcripts tested despite being non-polyadenylated, suggesting the presence of an alternative method for stabilizing these RNAs.

Acknowledgements

I would like to thank my advisor, Dr. Michael Schmale, and my committee members, Dr. Nevis Fregien and Dr. Marjorie Oleksiak, for their time, advice, and assistance on this project. I would also like to thank my lab members, Dayana Vidal, Pat Gibbs, and Merly Ovares for their advice and expertise during these last three years. Finally, I would like to thank Justin Greer and Nick Kron for their time discussing qPCR methods with me.

TABLE OF CONTENTS

Page

List of Figures

List of Tables

Chapter 1- Introduction

Bicolor damselfish (*Stegastes partitus*) are a tropical species found throughout the Caribbean as well as on South Florida reefs. Some bicolor damselfish found on the South Florida reefs have been documented to be affected by a naturally-occurring, transmissible, and fatal tumor causing disease termed Damselfish Neurofibromatosis (DNF) (38). This disease shares some characteristics with human Neurofibromatosis (Type 1), which makes the bicolor damselfish an excellent model for studying of this disease (36, 38). Damselfish Neurofibromatosis progresses through five defined cancer stages with death occurring as early as stage three, although it may occur earlier or later than this point (38). The disease is marked by the development of tumors in the Schwann cells (neurofibromas and malignant peripheral nerve sheath tumors), and chromatophores (chromatophoromas), which cause pigmented lesions on the skin of the damselfish. The tumors are highly invasive and disseminate throughout the fish in natural cases. The neurofibromas usually become malignant in DNF, unlike the tumors caused by human neurofibromatosis (36, 37, 38). Human Neurofibromatosis is an inherited autosomal disease, so prior work was conducted to determine how DNF is transmitted. Schmale discovered that the disease was found at a higher prevalence on reefs with denser populations of damselfish (36). Given that bicolor damselfish are territorial species and highly aggressive, the observations seen in the previous paper led to the hypothesis that DNF was being passed horizontally through fish to fish contact rather than genetically as in the case of Human Neurofibromatosis. However, vertical transmission was not completely ruled out as a possible mode of transmission. The hypothesis that DNF was

being passed through horizontal transmission was then tested through laboratory experiments and verified (37).

Schmale (37, 38) showed that injection of tumor homogenates, cultured tumor cells, or cell free filtrates were all capable of causing tumor development in healthy fish. The success of the cell free filtrates in causing tumors suggested that a sub-cellular agent was being released that was tumorigenic. This discovery gave rise to the hypothesis of a virus as the cause of DNF as some DNA and RNA viruses have been shown to cause tumors (37). A 2.4 kb DNA was found to be directly associated with the tumors and tumorigenicity of injected material (39). Yet, no distinct particle has been identified and, thus, this material was termed the damselfish virus-like agent or DVLA. Rahn et al (32) conducted a study to determine the RNA transcript patterns following DNase treatment in each of the tumor cells lines. Up to five DVLA transcripts (0.3, 0.5, 0.8, 1.0 and 1.4 kb) were identified from northern blots of tumor-derived cell lines and tissues. Concentrations of the transcripts vary between cell lines particularly with the smallest and largest transcripts (32). Further experiments were done to identify that DVLA DNA and RNA are located within the mitochondria of the cells, but the exact mechanism of its transcription is not yet known.

Mitochondria have become a target of interest recently due to their role in the development of many diseases including cancer, diabetes, and Alzheimer's. These diseases are usually due to some defect in mitochondrial functioning. This is caused by the wide number of functions that the mitochondria participate in, including the formation of ATP, apoptosis, metabolism, and pathogen recognition (4, 7). Mitochondria have a double membrane structure and transcribe some of their own genes in addition to

using nuclear transcribed genes for proper functioning. The RNAs transcribed directly within the mitochondria are transcribed from the heavy and light strands of the genome. The heavy strand has two promoter sites and transcribes 12 mRNAs, 2 rRNAs, and 13 tRNAs, while the light strand has one promoter that transcribes the ND6 mRNA of complex I and 8 tRNAs (8, 13). Proteins translated from the 13mRNAs are used exclusively for oxidative phosphorylation (4, 7, 29, 30). The d-loop region of the human mitochondrial genome is responsible for the initiation of transcription and DNA replication and is regulated by nuclear encoded proteins that are transported to the mitochondria. Mitochondrial transcription operates through use of three separate components: 1) the mitochondrial RNA polymerase, 2) mitochondrial transcription factor B2, and 3) mitochondrial transcription factor A. These three protein components are nuclear encoded. However, the mechanisms for transcription and processing will vary between species of different phyla despite the mitochondria arising from a monophyletic origin (4, 20, 29).

Unlike the other eukaryotic RNA polymerases, the mitochondrial polymerase is composed of just one subunit that is closely related to bacteriophage RNA polymerases and, in the case of the mitochondrial RNA polymerase, cannot initiate transcription on its own. The mitochondrial RNA polymerase is also involved indirectly in oxidative phosphorylation because it transcribes important subunits in complexes I, III, IV, and V of the electron transport chain, while the subunits of complex II are entirely nuclear encoded. It has also been recently discovered that there is a fourth nuclear RNA polymerase that exhibits similarities to the mitochondrial targeting RNA Polymerase (28). This polymerase is known as spRNAP-IV and has been shown to transcribe some

nuclear genes that are resistant to RNA polymerase II inhibition including the mitochondrial RNA polymerase gene. SpRNAP-IV and mtRNAP are both transcribed from POLRMT gene but the former is missing the N-terminal region that targets the protein to mitochondria (28). Overexpression of the mitochondrial polymerase has been identified in numerous hematologic malignancies and has also been associated with the promotion of tumor growth in breast cancer (8). Blocking of transcription by the mitochondrial RNA polymerase can be accomplished with nucleoside reverse transcriptase inhibitors, antiviral ribonucleosides, and ethidium bromide (4, 6). After mRNA is transcribed in the mitochondria, it usually becomes mature by undergoing polyadenylation by poly (A) polymerases, which play a key role in determining the stability of mitochondrial mRNA especially among distinct species. This process creates a poly (A) tail of approximately 50 adenylates and is used as a stabilizer in human mitochondria as it ensures that proper STOP codons are in place; however, in plants and bacteria this process leads to a more rapid degradation process of the mRNAs (7, 9, 20, 30). In the case of oculopharyngeal muscular dystrophy, the earliest defect detected was a down-regulation of the mRNAs encoding the mitochondrial proteins which was caused by shorter poly-A tail lengths. This defect was documented in *Drosophila*, mice, and humans and could be improved by reducing the deadenylation of these mRNAs (10). In *Trypanosoma brucei*, polyadenylation has different effects depending on if the mitochondrial RNAs are edited or unedited and are regulated throughout their life cycle for some mRNAs. A poly (A) tail on unedited mitochondrial RNAs causes a more rapid degradation, while a short or long poly (A) tail on partially edited or fully edited mitochondrial RNAs decreases the rate of degradation (26). Rahn's unpublished

dissertation data show that DVLA RNAs are probably NOT polyadenylated to any significant degree. This would suggest that these RNAs would have a shorter half-life compared to the poly-adenylated RNAs.

Control of mRNA turnover is crucial for proper gene expression and the removal of improperly formed mRNA has been looked at by numerous studies (6, 20, 30). Mitochondrial mRNA turnover and stability is the focus of the first aim by looking at the half-life differences between DVLA loop and DVLA stem. Typically, RNA half-lives are measured by inhibiting transcription using a compound such as actinomycin D and then measuring the degradation over several time points. To investigate the mitochondrial mRNA stability in Hela cells, Piechota et al (30) measured half-lives by blocking transcription and measuring steady state levels. They determined that the steady state level was determined by several factors including excision efficiency, defective transcripts, and the interaction with RNA-binding proteins. Borowski et al (7) identified the enzyme, hSuv3p, as a major component of mitochondrial mRNA turnover in humans. This enzyme, as they reported, served three functions including half-life maintenance and degradation of improperly formed transcripts. It has also been shown that transcripts involved in transcription regulation and signal transduction tend to have shorter half-lives compared to those responsible for metabolism, and protein translation and degradation (19). Piechota et al (30) investigated the half-lives of several mitochondrial mRNAs and showed that this measurement varied from one to seven hours for the ones tested. Furthermore, Friedel et al (19) showed that half-lives varied with function and within families. They showed that some mitochondria half-lives were near sixteen hours and for one protein family, in humans, the range varied from one to thirty-eight hours. Half-life

measurements have also been shown to be similar in conserved genes from species to species at least in the case of mammals (19).

In addition to the work done on mitochondria alone, high interest has also been placed on viruses that utilize mitochondria to aid in their replication either through triggering apoptosis, hindering apoptosis, or disrupting other essential mitochondrial functions. Both DNA and RNA viruses utilize host cell components; although this occurs to different extents based on the virus itself. Furthermore, different families of viruses use different areas of the host cell to aid in their transcription and replication. Some will disrupt macromolecular synthesis of the host cells as seen with the coronavirus and mouse hepatitis virus, while others will target the mitochondria directly. DVLA has not been characterized as an actual virus now but may behave similarly to viruses particularly small DNA viruses, mitoviruses, or plasmids.

The virus family *Nodaviridae* contains the alphanodaviruses, which infect insects and mammals, and the betanodaviruses, which infect fish. Both subgroups of the viruses have been shown to interact with the mitochondria of various organisms (22, 24, 42). The Nodamura virus, from the alphanodaviruses, has been shown to cause changes in mitochondrial membrane arrangement and mitochondrial localization through the interaction of its RNA dependent RNA polymerase with the outer mitochondrial membrane (22). The betanodaviruses affect mitochondria by triggering ROS production, and reducing mitochondrial membrane potential. This is all caused by the B2 protein and triggers apoptosis within the cells. The B2 protein targets the mitochondria via a specific sequence at the N-terminal end of the protein. It increases the production of hydrogen peroxide in fish cells, human cancer cells, and embryonic zebrafish cells to trigger an

oxidative stress response, which can be alleviated by treatment with antioxidants such as N-acetylcysteine (NAC). The B2 protein also causes fragmentation of the membrane by localizing Drp1, a mitochondrial fission protein, to the mitochondria (24, 42).

Rubella virus, an enveloped, single-stranded RNA virus stimulates apoptosis of infected cells through several mechanisms. This virus will utilize its C protein through the intrinsic apoptosis pathway of the mitochondria to interact with pro-apoptotic proteins like p32 and p53. Rubella starts the apoptosis process by increasing permeability by opening the mitochondrial permeability transition pore, which then triggers the migration of the apoptosis-inducing factors to the nucleus as well as the release of cytochrome C into the cytoplasm. Rubella virus will also shuttle p53 away from the mitochondria and to the nucleus to trigger apoptosis and release the virus to spread further (12). This demonstrates how a virus can manipulate many features that were originally meant to protect the cell against viral replication but are instead used to aid in the replication and survival process of the virus. In contrast to rubella virus, West Nile virus does not induce apoptosis purposely but instead is recognized by the innate immune system properly, so that the spread of the virus is inhibited by mitochondrial driven apoptosis (44). Another good example of a virus attacking mitochondria can be seen with the herpes simplex virus (HSV). The virus has been shown to deplete nuclear encoded mRNAs upon infection so that the viral mRNAs can take over. However, HSV infection was also discovered to cause complete degradation of mitochondrial DNA. One HSV protein known as UL 12.5 has been shown to localize to the mitochondria and is believed to be the cause of the degradation of both mitochondrial DNA and mitochondrial mRNA in infected cells although the process for mitochondrial mRNA has not been identified (35).

Walleye Dermal Sarcoma virus is a retrovirus that affects multiple areas of the cell during the disease progression in fish. This disease proceeds in a seasonal pattern of tumor formation and regression. The virus contains three unique open reading frames, *orf*a, *orf*b and *orf*c that encode three key viral proteins. *Orf*a and *Orf*b, located in the nucleus and plasma membranes respectively, are found in the developing tumors when viral gene expression is low. These two regions are responsible for inhibiting viral replication and stimulating cell proliferation for tumor development. During spawning, there is an increase in viral gene expression and in *orf*c protein expression. The *orf*c protein has been shown to associate with the mitochondria and causes a decrease in mitochondrial membrane potential to trigger apoptosis of the fully developed tumors. This allows for the transmission of the virus through the water column to naive fish at the spawning site (33, 34).

The following examples may behave more like DVLA than the animal viruses above in relation to how they interact with the mitochondria. Akins et al (2) used a plasmid found in a fungus (*Neurospora crassa*) instead of a virus to affect the mitochondria. In this report, the authors demonstrated that suppressive and defective mitochondrial plasmids of *Neurospora* can outcompete the wild type mitochondrial DNA and integrated themselves into the host's mitochondrial DNA. The mechanism by which this occurred was through disrupting protein synthesis in the mitochondria thus affecting the mitochondrial DNA stability (2). Another similarly behaving virus is a subset of the mycoviruses found in fungi known as mitoviruses. They are termed mitoviruses because they reside and replicate inside the mitochondria of the fungal host. Mitoviruses are dsRNA viruses that encode their own RNA- dependent RNA polymerases and use the

mitochondrial codon system rather than the universal cytoplasmic codon system. These mitoviruses also exhibit horizontal transmission through hyphal anastomosis and in some cases, reduce the virulence of the host species (23). However, some RNA viruses still rely on specific host cell factors to operate their own RNA dependent RNA polymerases (17, 27). Some viruses will even incorporate host cell proteins into their RNA-dependent RNA polymerases as seen with some polioviruses that have been shown to incorporate the host's translation elongation factor alpha, EF-1α (27). Because DVLA has not been found to encode any transcription factors or proteins, this suggests that DVLA is utilizing the mitochondria's own DNA replication and transcription processes to carry out its own transcriptional process.

Although much research has been conducted over the years on mitochondria and some on viruses affecting mitochondria, there has been very little work involving viruses or virus-like agents found within the mitochondria since there have been no other infectious agents of the mitochondria discovered in animals. Therefore, understanding the mechanism by which DVLA is transcribed within the mitochondria as well as how it affects the host mitochondria is necessary. To better understand where DVLA RNA is being transcribed, different transcription inhibition experiments were conducted. RNA Polymerase II transcription was inhibited first with alpha-amanitin and then with Triptolide to see how DVLA would be affected. Additionally, mitochondrial RNA transcription was inhibited by treatment with ethidium bromide to see how DVLA RNA would be affected. This research could expand our knowledge on novel mechanisms by which viruses cause disease, cancer, and utilize host cell components.

Chapter 2- Methods

Cell lines and Cell Culture

Immortalized DVLA positive and DVLA negative damselfish cell lines were created from tumored and healthy fish respectively. The DVLA positive cell lines used were 86-583, 88-503, 89-734, 92-16, and 96-24. The DVLA negative cell lines used were 63L, 77B, 22A, and FB3. The origin and preparation of these cell lines was described previously (37, 39). The cell lines were cultured at 28°C in complete Leibovitz's L-15 media with 10% Fetal Bovine Serum, 10% sterile water, additional NaCl, 5mL of Streptomycin, Penicillin, Amphotericin B mix added to each 500mL bottle with pH adjusted to 7.55-7.60. Prior to use 6mL of Ampicillin, 10mg/mL, was added to each bottle of media.

RNA preparation and qPCR

At the end of each experiment, the cells were harvested by removing the old media and replacing it with 5-10 mL of fresh, complete L-15 media. The cells were then immediately scraped off the bottom of the flasks and transferred into 15 or 50 mL blue max tubes and spun down for five minutes. The media was discarded, the cells were lysed with 750 µl of TRIzol, and the RNA extracted using the TRIzol Reagent Protocol from Ambion. The RNA was DNased using the Turbo DNA-free procedure (Ambion) and made into cDNA with either GoScript cDNA kit (Promega) or SuperScript III cDNA kit (Ambion). The cDNA was analyzed by qPCR and tested for the expression levels of β-actin, EF1-α, 18S, cytochrome-b, D-loop, DVLA loop, and DVLA stem. The sequences for each primer set is listed in table 1 below. Nuclear gene primers were

created from the *Stegastes partitus* genome by using NCBI BLAST tools while the DVLA and mitochondrial gene primers were created from previously obtained genome sequences. The thermal profile for the qPCR was set for 1 cycle at 95°C for 10 minutes, fifty cycles of 30 seconds at 95°C, 30 seconds at 60°C, and 30 seconds at 72°C, and 1 cycle of 1 minute at 95°C, 30 seconds at 55°C, and 30 seconds at 95°C for melting point analysis. The qPCRs were conducted using the MxPro program on a Stratagen Mx3005 machine with the Sybr Green fluorescent dye.

Table 1: Sequences of transcripts. Shown are the primer pair sequences for all genes used throughout the experiments.

Gene	Forward Primer	Reverse Primer
β-Actin	5'-atgtggatcagcaagcagga-3'	5'- tgcacagagcggaagttgtt-3'
EF1-α	5'cccggtatggtcgtcacctt-3'	5'-cgacggatttccttgatggac-3'
18S	5'-tagaggtgaaattcttggacc-3'	5'-ggatcgctagttgggatcg-3'
Cytochrome-b	5'-gttctcagtagacaacgccac-3'	5'-gtcctactgggttgtttgatcc-3'
D-loop	5'-gcttacattgactaatgtttgc-3'	5'-atgagtttacactgtgaaatgc-3'
DVLA loop	5'-accagcgttctcagtcatcg-3'	5'-cagtcctcttctaatatctgagc-3'
DVLA stem	5'-gtcaccacccactaatctatc-3'	5'cgtggcacctcaaatgttcc-3'

4-Thiouridine RNA Synthesis labeling

RNA synthesis was measured by following a protocol described by Radle et al. (29) using 4-thiouridine (4sU) to label newly synthesized RNA. The cells were plated at a concentration of 4 million cells per T-75 flask with three flasks per time-period. Each flask was treated with 200 μM 4sU in five mL of media for two or six hours. At the end of the labeling period, the cells from replicate flasks were harvested and pooled together.

The RNA was extracted following a modified TRIzol RNA extraction protocol. Eighty μg of the RNA was biotinylated with HPDP-Biotin during an hour and a half incubation period with rotation. HPDP- Biotin will bind to the RNA that has incorporated the 4sU and will represent the newly transcribed fraction of the RNA. The biotinylated RNA was incubated with streptavidin coated magnetic beads for fifteen minutes with rotation and was then added to magnetic columns to separate it into newly transcribed and pre-existing RNA fractions. Each fraction was DNased and made into cDNA and analyzed via qPCR with the primers for β-actin, EF1-α, DVLA loop, DVLA stem, cytochrome-b, and d-loop. The percentage of newly transcribed RNA to the total, which is made up from the new fraction plus the pre-existing fraction, was used to calculate the percent new synthesis for each gene. Total RNA copy numbers for each transcript were calculated by taking the copy numbers for the whole sample of the new fraction and adding it to the copy numbers for the whole sample of the pre-existing fraction. This number was then divided by the total amount of RNA to get copies per ng of RNA. The total amount of RNA was calculated as the amount of new RNA plus the amount of pre-existing RNA. Estimated half-life calculations were also derived by using percent new RNA synthesis. The equation used to calculate half-life was $-t\ln(2)/\ln(1-\text{percent new synthesis})$ where t equals the incubation time with the 4sU label. A steady state system was assumed during the duration of the assay.

RNA polymerase II Transcription Inhibition with alpha-amanitin

RNA transcription was tested by treatment with alpha-amanitin, a known RNA polymerase II inhibitor (Figure 1). Five immortalized tumor cell lines were used in the

alpha-amanitin inhibition experiments including 86-583, 89-734, 88-503, 92-16, and 96-24. Each cell line was plated into T-25 flasks at a concentration of four million cells per flask. Each cell line was tested with two exposure times: twenty-four hours and forty-eight hours. Two drug dose levels were tested with each cell line at each testing period duration. These concentrations used were 0.1, 1.0 and 5.0 µg in 5 mL of freshly changed complete L-15 media. Three biological replicates were used for each round of treatments. The effects of alpha-amanitin were also tested using the 4sU synthesis method described above. The cell lines 89-734 and 86-583 were plated into T-75 flasks at a concentration of four million cells per flasks. The flasks were treated with 1µg of alpha-Amanitin in 5mL of complete L-15 media for either three or six hours prior to adding in the 4sU label.

RNA Polymerase I	RNA polymerase II	RNA Polymerase III	Mitochondrial RNA Polymerase
• Eukaryotic Nucleolus • Transcribes 18S, 28S, and 5.8S rRNAs	• Eukaryotic Nucleoplasm • Transcribes most mRNAs • Inhibited by low concentrations of α-Amanitin B-actin EF1-a	• Eukaryotic Nucleoplasm • Transcribes tRNAs, 5S, and small RNAs • Inhibited by high concentrations of α-Amanitin	• Inner membrane of the mitochondria • Transcribes all mitochondrial RNAs Cytochrome b D - loop

Figure 1:Four main RNA polymerases found in eukaryotic cells. The polymerase targeted for inhibition are identified by the drug of choice. Genes to be affected are also listed.

RNA polymerase II transcription Inhibition with Triptolide

Nuclear RNA Transcription was also inhibited by treatment with 0.1 µM and 1 µM triptolide, an RNA polymerase II inhibitor as seen in Figure 2. After initial experiments, the 1 µM dose treatment was dropped as it was too strong of a dose to measure RNA synthesis changes before complete transcription shutdown. RNA synthesis

was measured using the 4-thiouridine method described above. Both tumor and healthy cell lines were utilized. The tumor cell lines used were 89-734, 86-583, 96-24, and 88-503. The healthy cell lines used were 63L, 77B, 22A, and FB3. To show reproducibility, 89-734 was tested three times with 0.1µM Triptolide. Each cell line was plated into three T-75 flasks at a concentration of 4 million cells per flask. The flasks were then treated with Triptolide twenty-four or forty-eight hours later depending on the confluence and appearance of the cells after plating. The flasks were treated for one hour with triptolide prior to adding in the 4sU label for six hours. 200µM or 400µM 4sU was used for labeling depending on the confluence of the cells. All three flasks, for each treatment, were pooled together and the RNA extracted following a modified TRIzol protocol described in Radle et al. (29). Fifty to eighty µg of RNA were used in the biotinylation and separation process as described above. The genes tested with the tumor cell lines were β-actin, EF1-α, cytochrome-b, D-loop, DVLA loop, and DVLA stem. The ones tested for the healthy cell lines were also the same minus DVLA loop and DVLA stem.

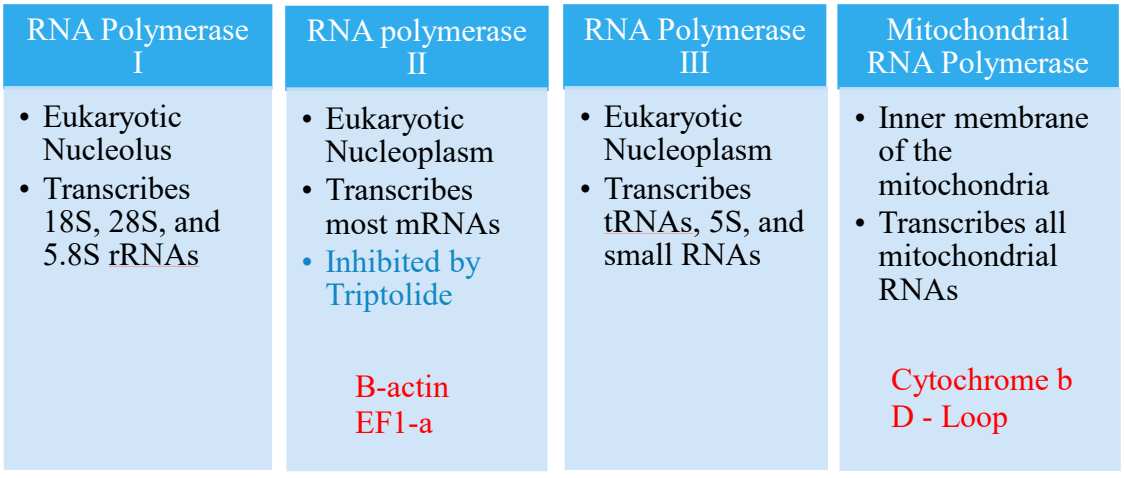

Figure 2: Four main RNA polymerases found in eukaryotic cells. The polymerase targeted for inhibition are identified by the drug of choice. Genes to be affected are also listed.

Mitochondrial RNA Transcription Inhibition with Ethidium Bromide

Two tumor cell lines, 86-583 and 89-734 were treated with varying doses of ethidium bromide (EtBr) to see if mitochondrial and DVLA gene transcription was inhibited as seen in Figure 3. RNA synthesis was measured by the 4sU method described above. Three T-75 flasks per treatment condition were plated with 4.5 million cells per flask. The doses used were 0 (control), 50nM, 100nM, and 500nM EtBr. All flasks were grown for seven days before the EtBr was added to 20mL of fresh complete L-15 media. After the EtBr was added, the flasks grew for another seven days. After seven days, all flasks were passaged and replated at 4 million cells per flask in 20mL of complete L-15 media with the appropriate dose of EtBr. The 4sU label was added to the flasks in 5mL of complete L-15 media 24hrs after the passage for 89-734 and 48 hours after the passage for 86-583. The time before the addition of the 4sU label was determined by the condition of the cells. The labeling time and harvest procedure was the same as with the Triptolide experiments described above. The data was then pooled together for statistical analysis.

RNA Polymerase I	RNA polymerase II	RNA Polymerase III	Mitochondrial RNA Polymerase
• Eukaryotic Nucleolus • Transcribes 18S, 28S, and 5.8S rRNAs	• Eukaryotic Nucleoplasm • Transcribes most mRNAs B-actin EF1-a	• Eukaryotic Nucleoplasm • Transcribes tRNAs, 5S, and small RNAs	• Inner membrane of the mitochondria • Transcribes all mitochondrial RNAs • Inhibited by EtBr Cytochrome b D - Loop

Figure 3: Four main RNA polymerases found in eukaryotic cells. The polymerase targeted for inhibition are identified by the drug of choice. Genes to be affected are also listed.

Data Analysis

The alpha-amanitin total RNA data were compared using the ΔΔCt values normalized to 18S for each individual flask. The data was normalized to 18S because it was predicted to be unaffected. In cases where 18S values varied from the control cultures, the other genes of the flask varied to the same extent as the 18S value which is why each flask was normalized to its specific 18S value prior to averaging. The ΔΔCt was calculated by subtracting the Ct of 18S from the Ct values of the other genes of the corresponding flask to get a ΔCt value. Mean ΔCt values were calculated across flasks for both the controls and the treatments. The ΔCt values of the treatments were then subtracted from the ΔCt of the controls for each gene to get the ΔΔCt value.

All data analyses were carried out using the SOFA statistics package. Synthesis percentages were calculated based on the copy numbers of a given gene and total RNA was defined as the new synthesis fraction plus the pre-existing fraction. Copy numbers were calculated based on conducting qPCR on plasmid standards for each gene. The plasmids were made from cloned PCR products for each primer pair in a TOPO TA vector. The standards were run in 10-fold dilutions from 1×10^8 to 1×10^4 in triplicate along with the calibrator made from 88-503 and an 89-734 sample to create a standard curve for each gene. The slope and intercept for each gene was then extrapolated to calculate the copy number per ng of RNA from the Ct values measured previously with the equation, Copy Number= EXP^((Ct-Intercept)/(slope)). For plates that had the calibrator sample present, the Ct was corrected by adding or subtracting the difference from the original 88-503 Ct value and the value on the current plate. This correction factor ranged from 0.02 to 1.0 and averaged to be 0.47. For experiments that did not have

the calibrator sample on the initial qPCR plates, the original Ct value was used in the copy number equation. Total RNA copy numbers were compared across tumor derived or healthy cell lines using a Kruskal-Wallace H test to determine that there were no statistical differences between the controls before pooling samples in these groups for further analyses. Correlations between the transcript copy numbers were evaluated using Spearman's R Correlation test. Differences in copy number between transcripts and between Healthy and Tumor cell lines were analyzed with a Mann-Whitney U test. The percent change in copy numbers of newly synthesized transcripts of each gene from the controls to the 0.1μM Triptolide treatments were calculated and compared using Mann-Whitney tests to evaluate differences across genes in the effect of Triptolide on new RNA synthesis. The same analysis was also used to evaluate the effects of EtBr across genes.

Chapter 3- Results

RNA Polymerase II Transcription Inhibition with alpha-amanitin

Alpha-amanitin inhibition of RNA synthesis was first investigated by measuring total RNA concentrations for twenty-four hours and forty-eight hours. Three drug dose levels, either 0.1, 1, or 5 µg in 5 mL of fresh L-15 media, were tested with each cell line at each testing period duration. After the initial tests with 89-734 and 86-583, only the 1 µg dose of alpha-amanitin was used because 0.1 µg was too low and 5 µg showed no major differences from the 1 µg dose (data not shown). Treatment with alpha-amanitin produced variable results as seen below in Figure 4. As predicted, both β-actin and EF1-α showed increased degradation consistent with the blocking of RNA polymerase II. D-loop showed an increase in expression levels and cytochrome-b showed an inconsistent pattern across experiments. DVLA loop showed a decrease in expression across most experiments while DVLA stem, like cytochrome-b, showed inconsistent results across experiments. The effect of alpha-amanitin on RNA synthesis measured using 4sU in 89-734 and 86-583 showed a strong exposure threshold between no apparent effect and complete inhibition of all RNA synthesis as shown in figures 5A and 5B. The cell line 89-734 showed complete shutdown of RNA transcription after three hours pre-treatment with alpha-amanitin (Fig 5A). 86-583 showed no RNA transcription inhibition after three hours pre-treatment and complete shutdown after six hours of pre-treatment with alpha-amanitin (Fig 5B).

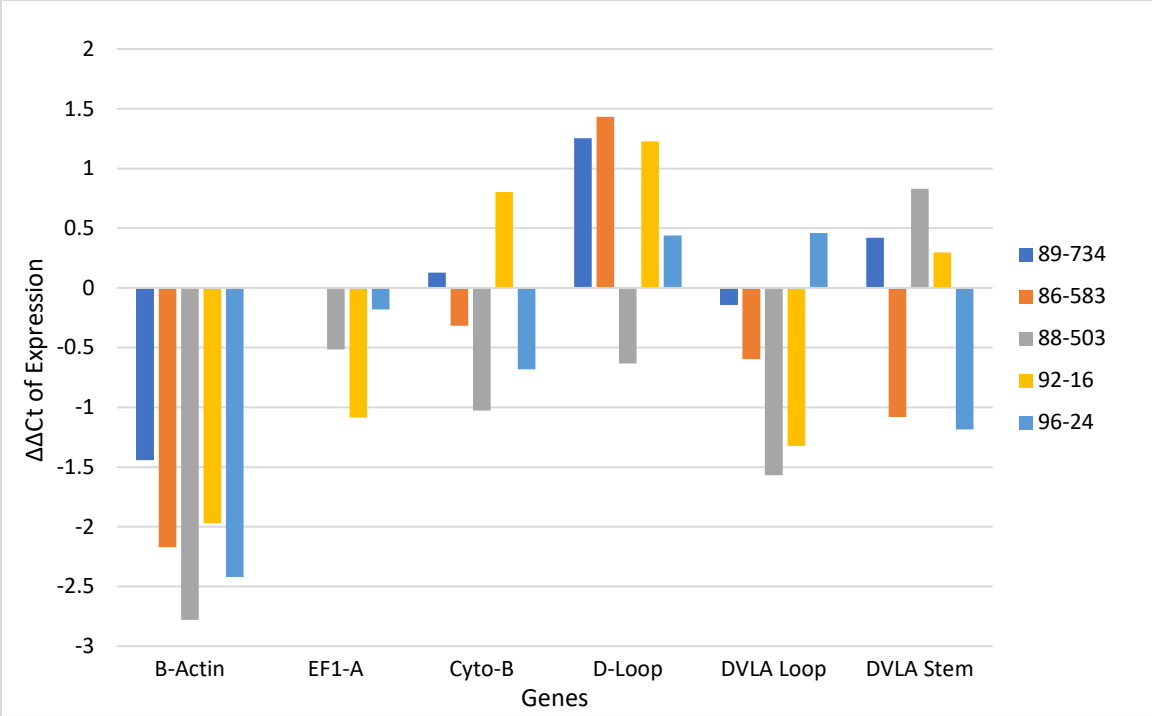

Figure 4: Change in transcript expression in tumor derived cell lines treated with 1ug Alpha-Amanitin for 24hrs to block RNA pol II transcription.

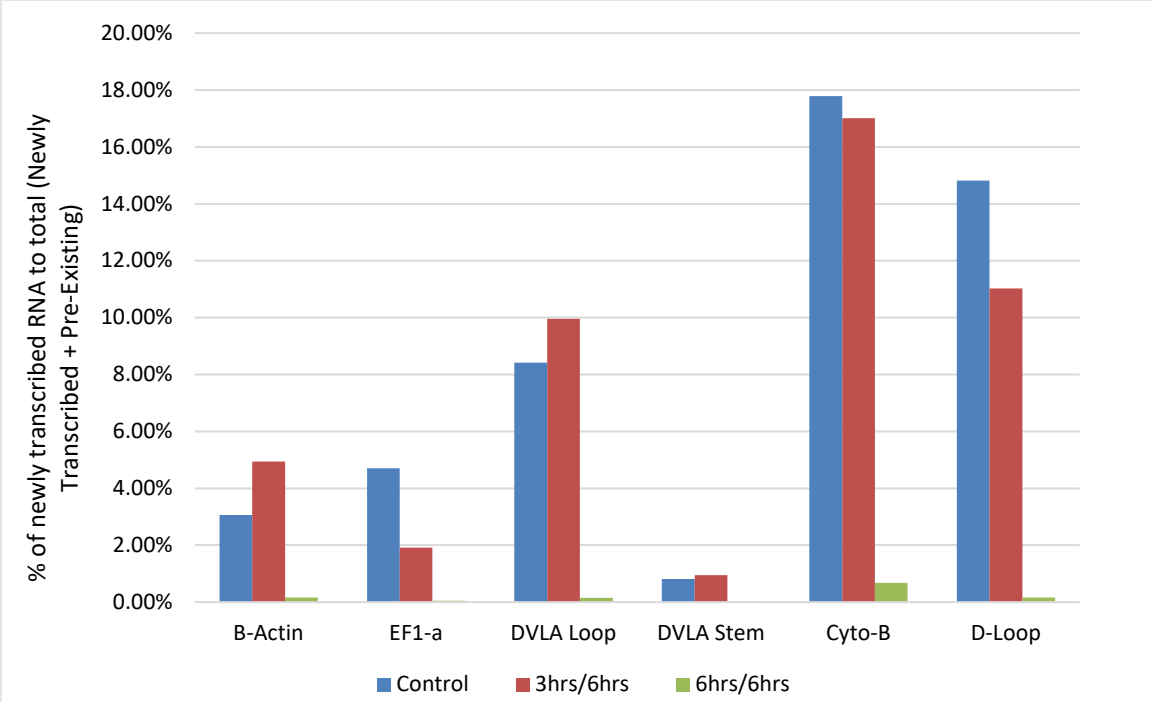

Figure 5A: RNA pol II transcription inhibition with 1 µg alpha-amanitin in 86-583. RNA synthesis was measured through 4sU labeling. Cultures were treated with alpha-amanitin for 3 or 6 hours prior to labeling with 4sU for 6 more hours.

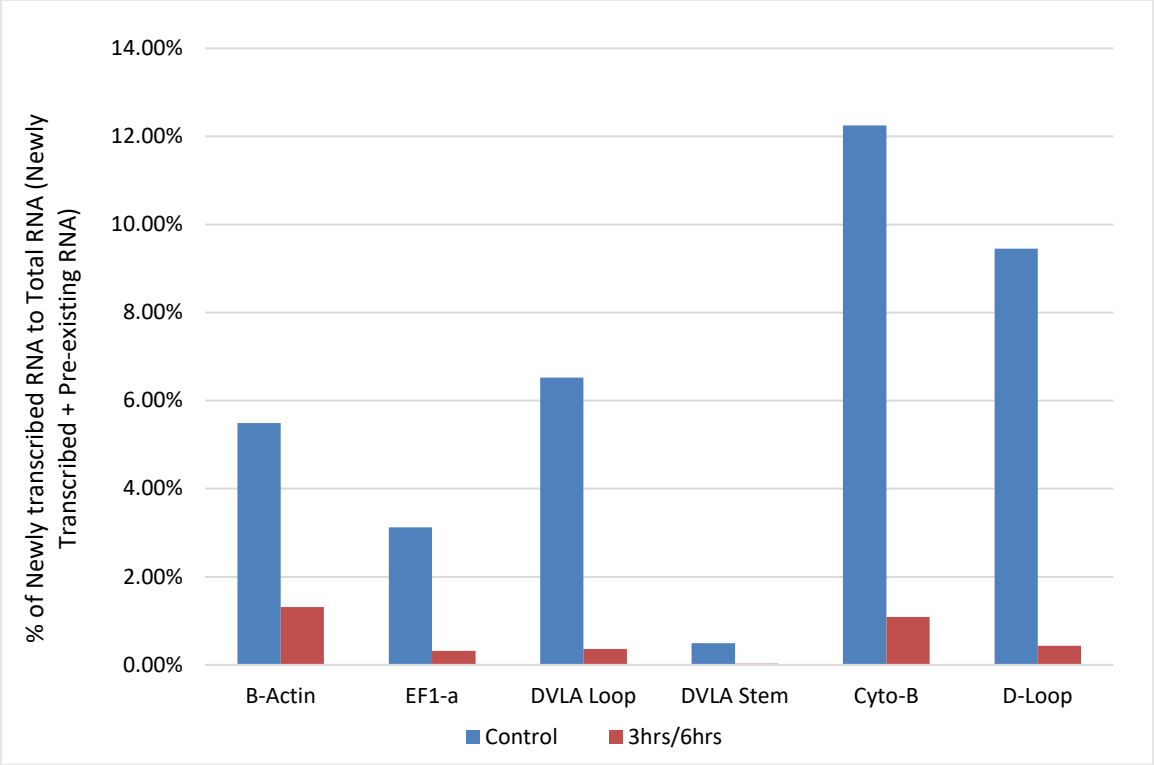

Figure 5B: RNA pol II transcription inhibition with 1 µg alpha-amanitin in 89-734. RNA synthesis was measured through 4sU labeling. Cultures were treated with alpha-amanitin for 3 or 6 hours prior to labeling with 4sU for 6 more hours

Total RNA transcript levels measured by 4sU labelling

There were no statistical differences in RNA copy numbers within cell lines from different experiments so total RNA copy numbers were averaged together by cell line as shown in Figures 6A-G with one gene per figure. There were also no significant differences in RNA copy number for any of the genes between the tumor and healthy cell lines. Figure 6A shows the averaged total RNA levels for all genes tested on a log scale. Statistical analysis of the total RNA copy numbers for all six-hour controls showed that β-actin and EF1-α have significantly greater copy number amounts per ng of RNA than the other genes tested in both tumor and healthy cell lines. Cytochrome-b and DVLA stem had the next highest copy numbers per ng of RNA of the genes tested. However, cytochrome-b had significantly less copy number amounts per ng of RNA than DVLA

stem ($p<0.01$, Mann-Whitney). Finally, D-loop and DVLA loop had the lowest copy number amounts per ng of RNA of all the genes and showed no significant difference from each other ($p>0.05$, Mann-Whitney).

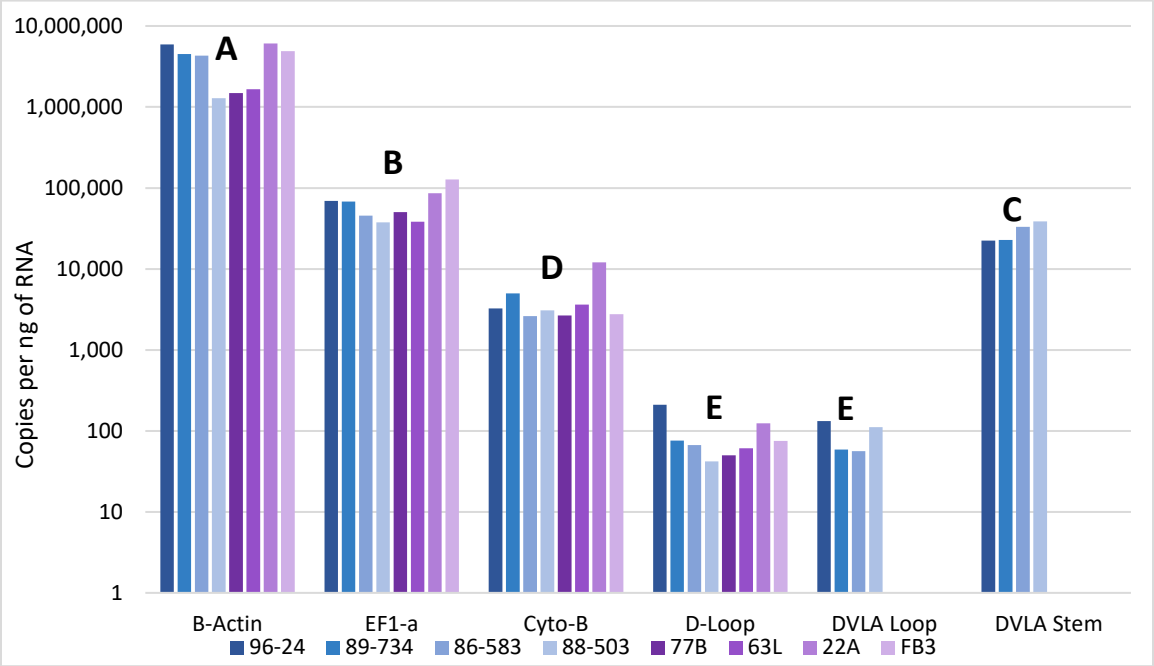

Figure 6A: Copies per ng of RNA for all genes. Copy numbers are grouped together by cell line and plotted on a log scale. Bars in blue represent tumor- derived cell lines and purple bars represent healthy cell lines. The letters above each gene shows which genes were significantly different from each other ($p<0.05$, Mann-Whitney U test). Same letters indicate no statistical difference. Sample size per cell line: 96-24=3, 89-734=6, 86-583=4, 88-503=1, 77B=2, 63L=2, 22A=2, FB3=1.

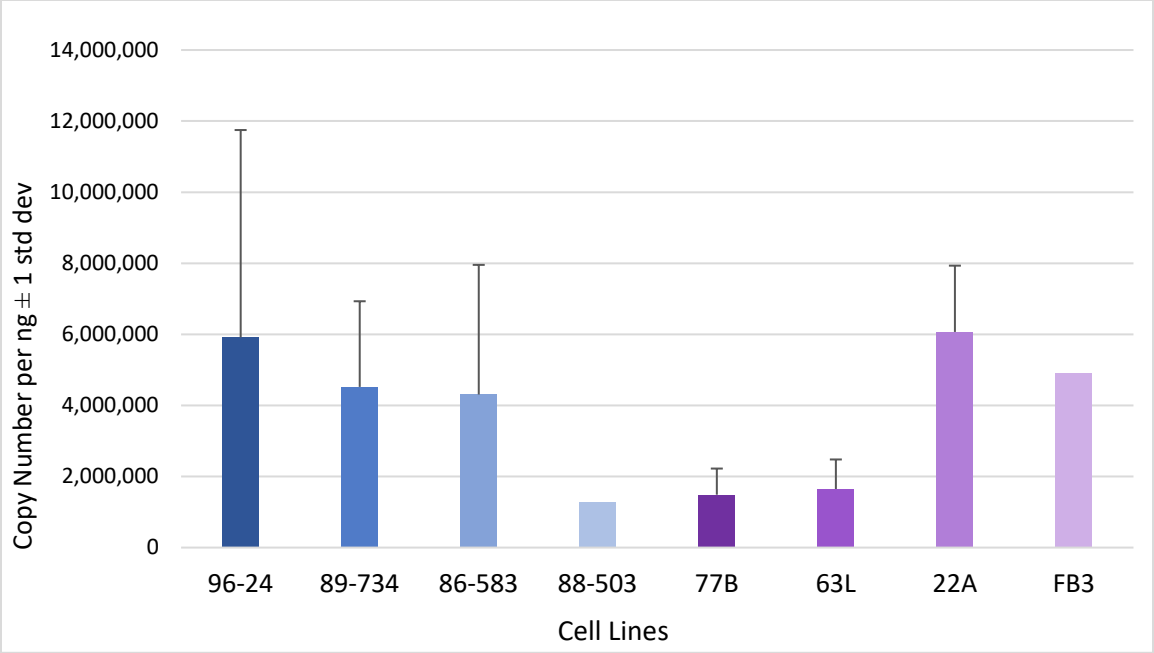

Figure 6B: Copies per ng of RNA for β-actin. Copy numbers are grouped together by cell line. Bars in blue represent tumor- derived cell line and purple bars represent healthy cell lines. Sample size per cell line: 96-24=3, 89-734=6, 86-583=4, 88-503=1, 77B=2, 63L=2, 22A=2, FB3=1.

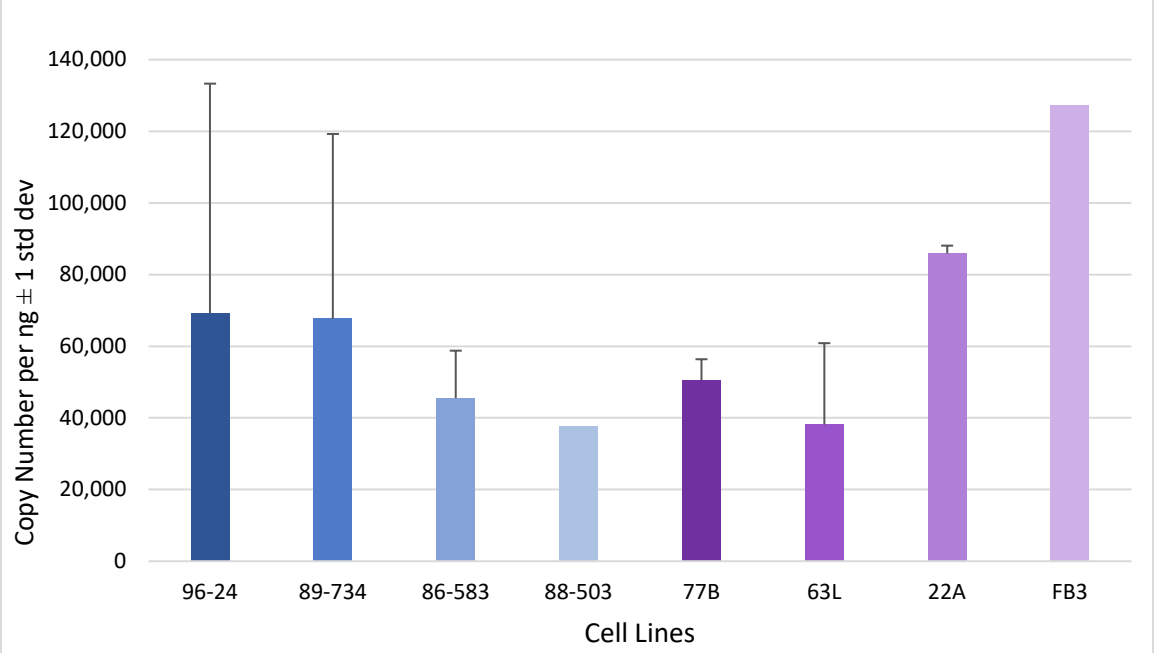

Figure 6C: Copies per ng of RNA for EF1-α. Copy numbers are grouped together by cell line. Bars in blue represent tumor- derived cell line and purple bars represent healthy cell lines. Sample size per cell line: 96-24=3, 89-734=6, 86-583=4, 88-503=1, 77B=2, 63L=2, 22A=2, FB3=1.

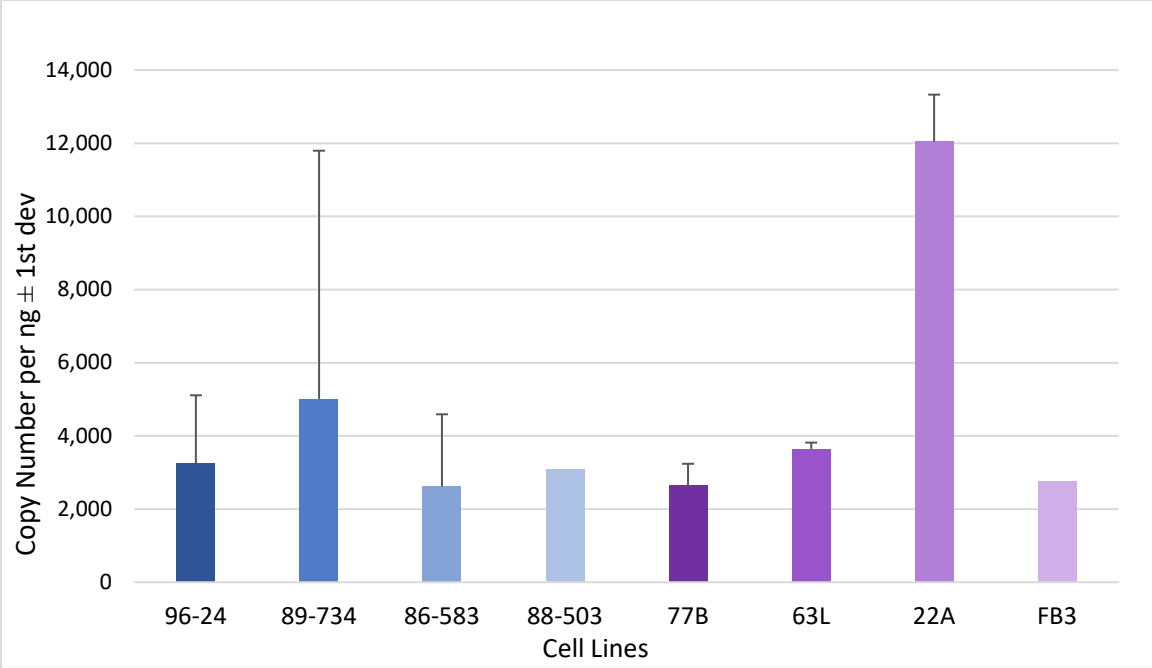

Figure 6D: Copies per ng of RNA for Cytochrome-B. Copy numbers are grouped together by cell line. Bars in blue represent tumor- derived cell line and purple bars represent healthy cell lines. Sample size per cell line: 96-24=3, 89-734=6, 86-583=4, 88-503=1, 77B=2, 63L=2, 22A=2, FB3=1.

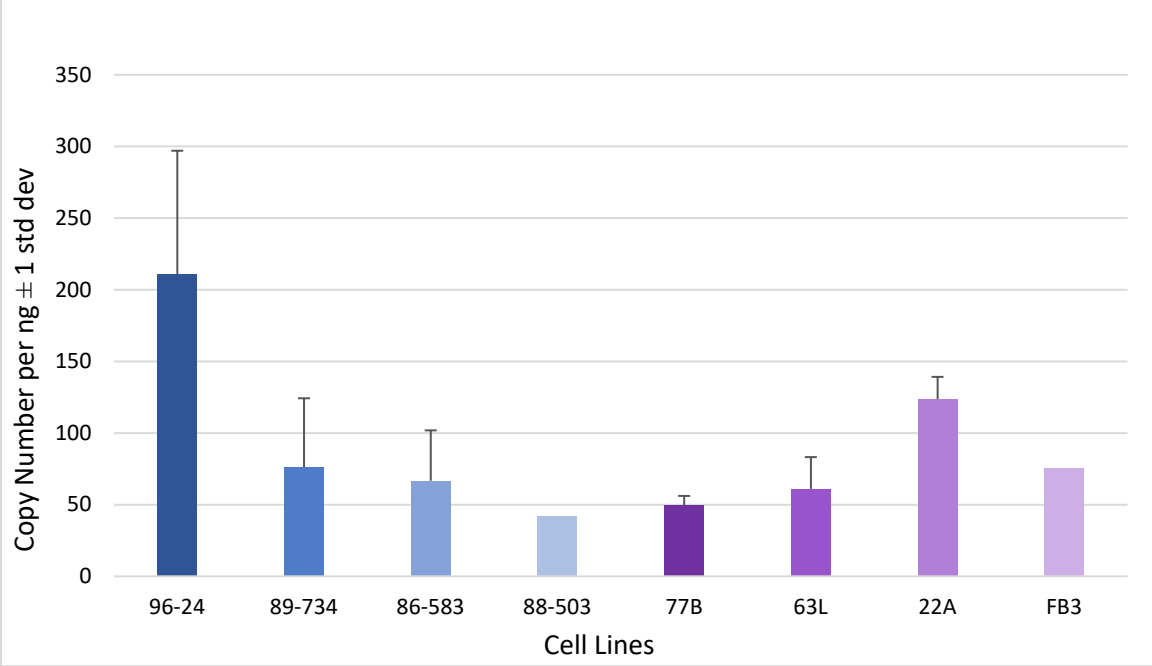

Figure 6E: Copies per ng of RNA for D-Loop. Copy numbers are grouped together by cell line. Bars in blue represent tumor- derived cell line and purple bars represent healthy cell lines. Sample size per cell line: 96-24=3, 89-734=6, 86-583=4, 88-503=1, 77B=2, 63L=2, 22A=2, FB3=1.

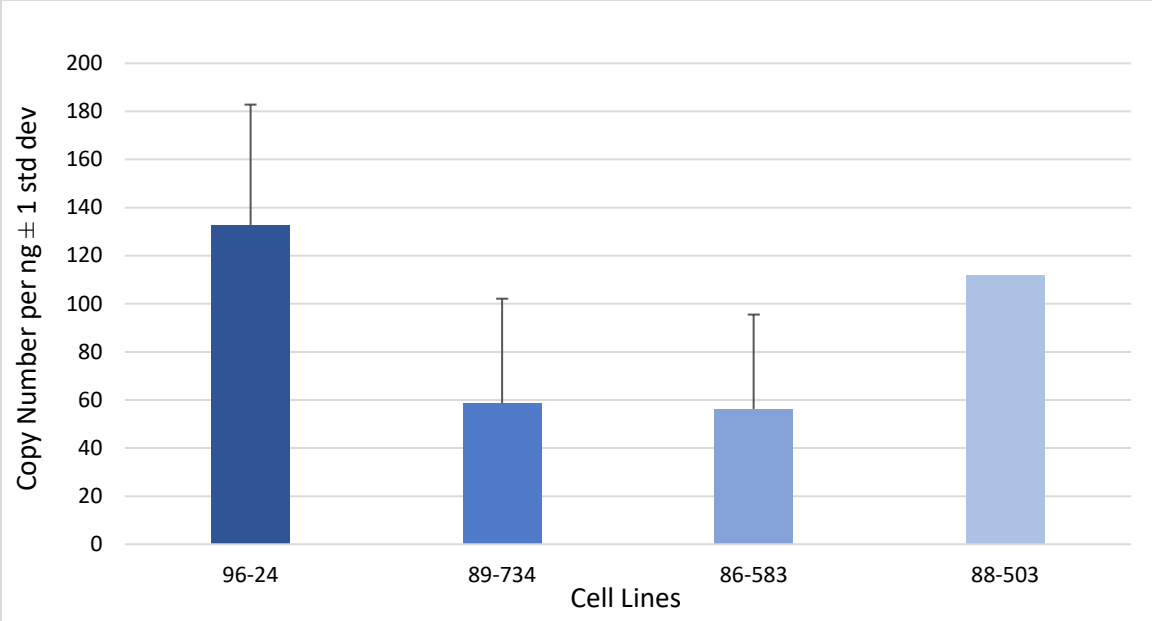

Figure 6F: Copies per ng of RNA for DVLA Loop. Copy numbers are grouped together by cell line. Bars in blue represent tumor- derived cell line and purple bars represent healthy cell lines. Sample size per cell line: 96-24=3, 89-734=6, 86-583=4, 88-503=1, 77B=2, 63L=2, 22A=2, FB3=1.

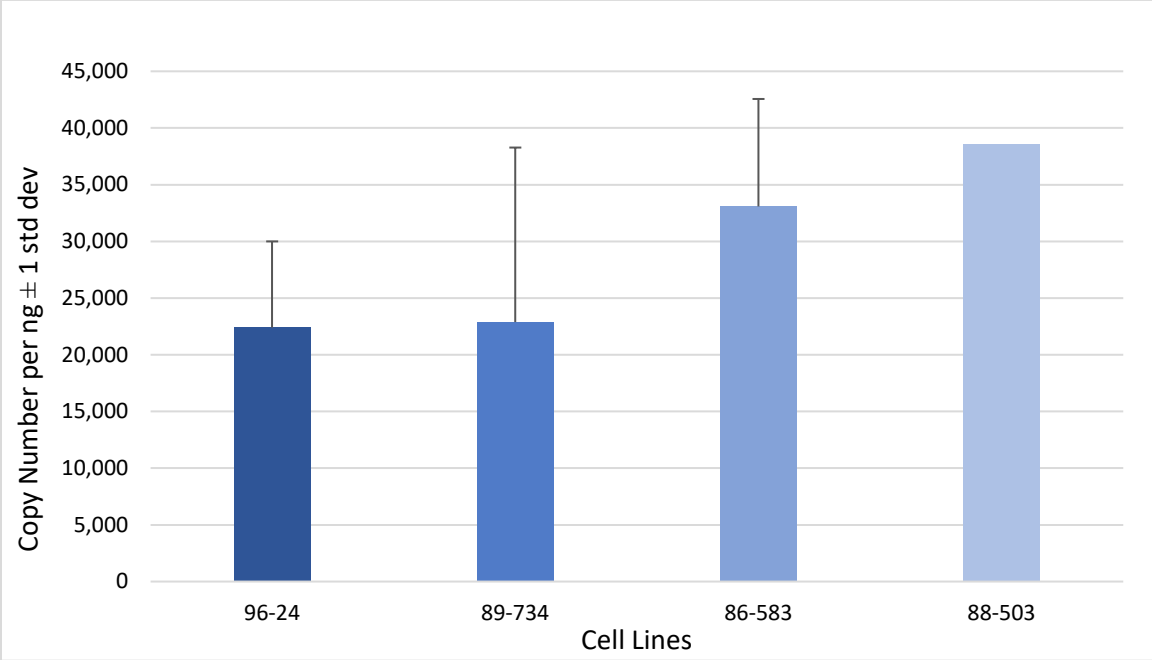

Figure 6G: Copies per ng of RNA for DVLA Stem. Copy numbers are grouped together by cell line. Bars in blue represent tumor- derived cell line and purple bars represent healthy cell lines. Sample size per cell line: 96-24=3, 89-734=6, 86-583=4, 88-503=1, 77B=2, 63L=2, 22A=2, FB3=1.

All statistically significant correlations between total RNA levels of RNA transcripts in the tumor cultures were positive. Table 1 shows the significant correlations in the tumor cell lines on top and the healthy cell lines on bottom. β-actin is positively correlated only to EF1-α in the tumor cell lines and is not correlated to any gene in the healthy cell lines. EF1-α is positively correlated only with cytochrome-b in the tumor cell lines. DVLA stem is correlated to cytochrome-b in the tumor cell lines, while DVLA loop is strongly correlated to both cytochrome-b and D-loop.

Table 2: Spearman's R Correlation Coefficient between total RNA transcript copy numbers. Tumor derived lines on top, Healthy cell lines on bottom.

	β-actin	**Ef1-α**	**Cyto-B**	**D-Loop**	**DVLA Loop**	**DVLA Stem**
β-actin		0.57*	-	-	-	-
EF1-α	-		0.63*	-	-	-
Cyto-B	-	-		0.69**	0.63*	-
D-Loop	-	-	-		0.62*	-
DVLA Loop						-
DVLA Stem						

- denotes a non-significant value

* $p<0.05$

**$p<0.01$

Furthermore, the new RNA synthesis copy number data were highly correlated as shown in table 2. β-actin showed significant positive correlations to all genes tested except for DVLA stem during RNA synthesis. All the mitochondrial and DVLA genes showed significant correlations to each other during synthesis unlike what was seen in the total RNA levels. In the healthy cultures, the nuclear genes were significantly correlated to each other as were the mitochondrial genes to each other.

Table 3: Spearman's R Correlation Coefficient between new RNA synthesis transcript copy numbers. Tumor derived lines on top, Healthy cell lines on bottom.

	β-Actin	EF1-α	Cyto-B	D-Loop	DVLA Loop	DVLA Stem
β-Actin		0.61*	0.72**	0.75**	0.63*	-
EF1-α	0.82*		0.58*	-	-	-
Cyto-B	-	-		0.59*	0.54*	0.55*
D-Loop	-	-	0.89**		0.71**	0.78**
DVLA Loop						0.85**
DVLA Stem						

- denotes a non-significant value

* $p<0.05$

**$p<0.01$

4sU labelled RNA Synthesis and Half lives across cell cultures

To determine the effectiveness of the 4sU method of measuring RNA synthesis in the fish tumor cell lines, some basic synthesis rate experiments were completed. Initial synthesis experiments determined that six hours labeling time was optimal for measuring new RNA synthesis across cell lines as seen in Figure 7. Percent new synthesis data across the transcripts of the pooled data were compared in Figure 8, and showed that in the tumor-derived cell lines β-actin has significantly less percent new synthesis than cytochrome-b and D-loop ($p< 0.05$, Mann-Whitney) and significantly greater synthesis than DVLA stem ($p< 0.01$, Mann-Whitney). EF1-α synthesis is significantly less than cytochrome-b, D-loop, and DVLA loop ($p< 0.01$, $p<0.01$, and $p<0.05$ respectively, Mann-Whitney) and significantly greater than DVLA stem ($p< 0.05$, Mann-Whitney). Cytochrome-b, D-loop, and DVLA loop synthesis are all significantly greater than

DVLA stem synthesis ($p < 0.01$, Mann-Whitney). In the healthy cell lines, β-actin still showed significantly less synthesis than D-loop ($p<0.05$, Mann-Whitney) but not a significant difference with cytochrome-b. EF1-α still showed significantly less synthesis than cytochrome-b and D-loop. There were no significant differences in these synthesis patterns between tumor-derived and healthy cell lines for all genes by Mann-Whitney analysis as seen in Figure 8 below.

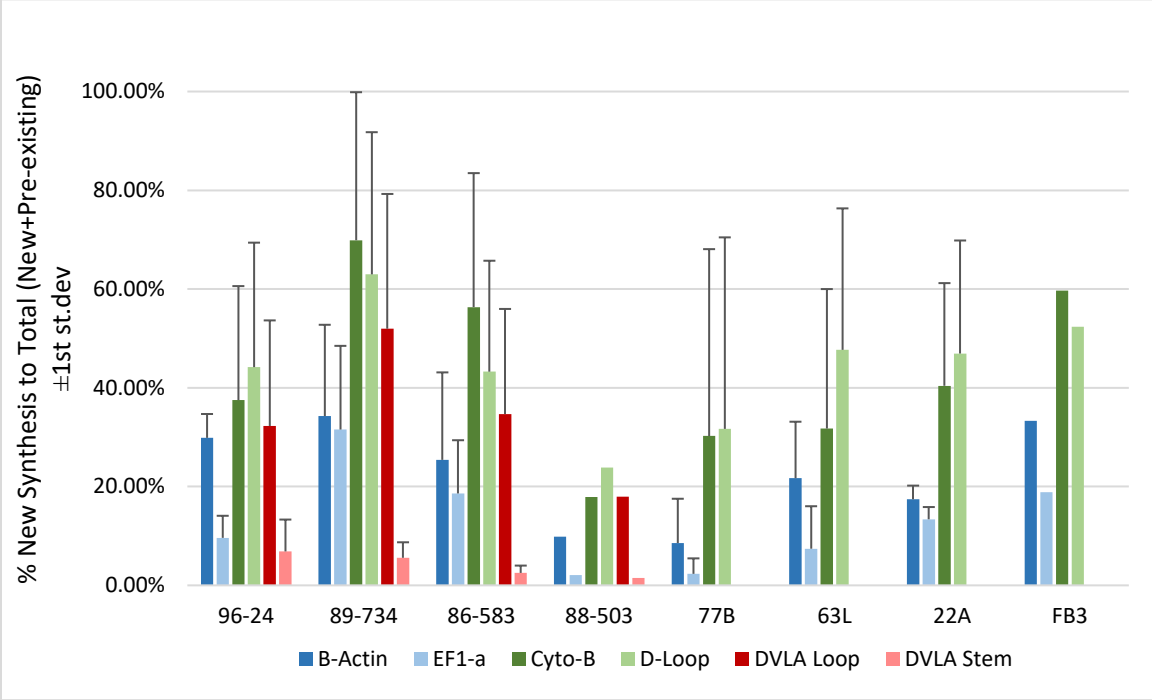

Figure 7: Percent New RNA synthesis to total for all 6hr control samples pooled together by cell line. Total is defined as the new fraction + the pre-existing fraction of RNA.

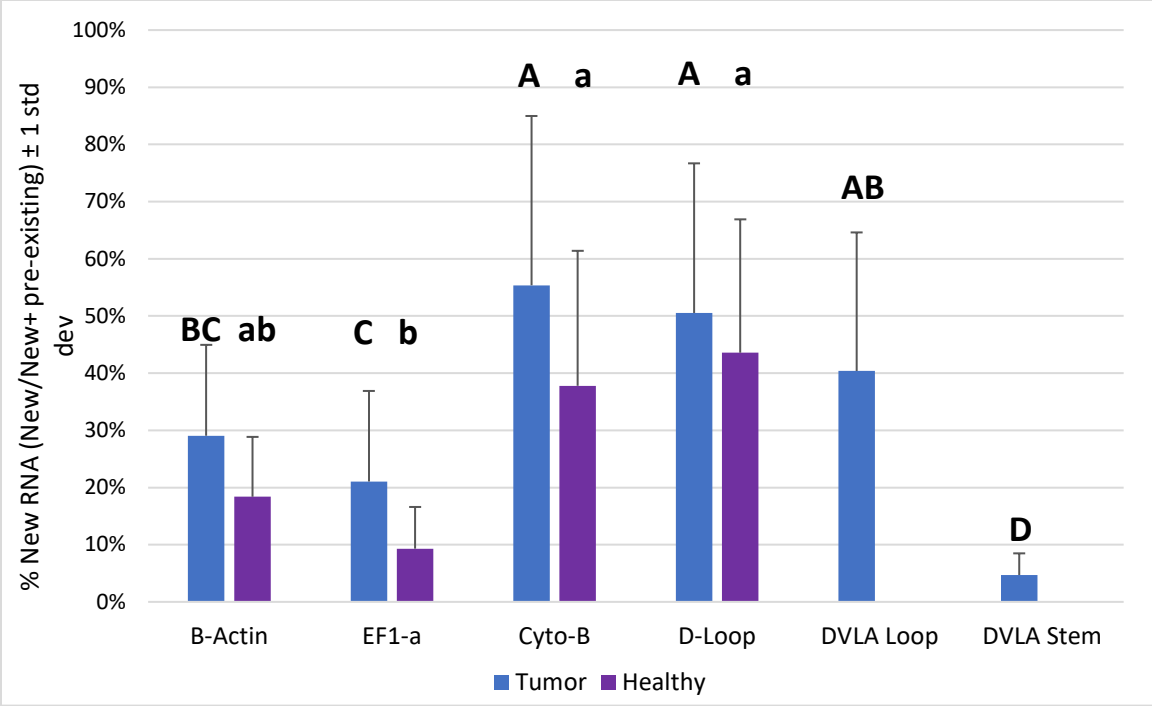

Figure 8: Percent new RNA synthesis after six hours incubation time for control samples only. Percent new RNA synthesis is calculated by the new fraction divided by the total. The total is defined as the new fraction plus the pre-existing fraction. . The letters above each gene shows which gene is significantly different from each other ($p<0.05$, Mann-Whitney U test). Same numbers mean there is no statistical difference. Upper case letters represent Tumor-derived cell lines and lower case letters represent healthy celll lines.

Percent new RNA synthesis was also used to estimate half-life times across the genes. The estimated half-life calculations for the tumor-derived versus healthy cell lines are shown in Figure 9. When a steady-state condition is assumed, cytochrome-b, D-loop, and DVLA loop all had half-life times of less than ten hours. The next longest half-life times were seen in β-actin and EF1-α, while DVLA Stem had the longest half-life of all the genes tested.

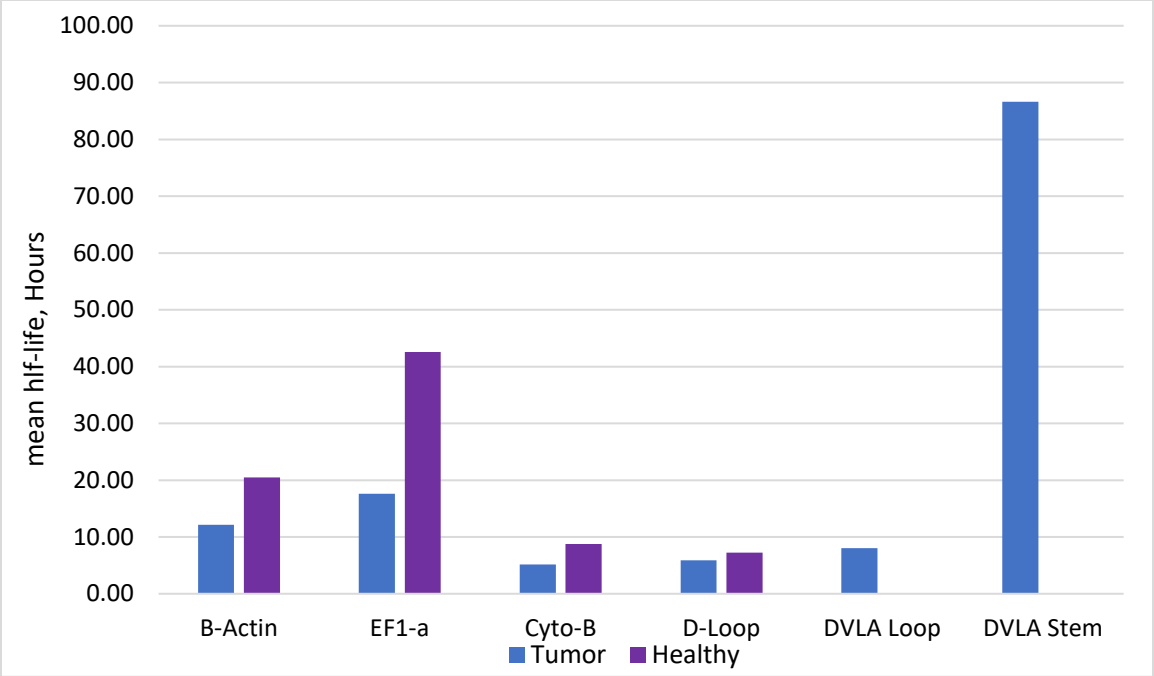

Figure 9: Estimated half-lives for each gene based on a six-hour incubation time, percent RNA synthesis and assuming a steady state situation. Pooled tumor-derived cell lines are plotted against pooled healthy cell lines.

RNA Polymerase II Transcription Inhibition with Triptolide

Determining RNA transcription inhibition by measuring RNA synthesis rather than total RNA concentrations was done due to the inconsistent results seen in the alpha-amanitin experiments. RT-qPCR results on several tumor and healthy cell lines showed a decrease in synthesis across all genes when treated with 0.1uM triptolide (figure 10). However, when the treatments were analyzed as a percent change in new synthesis of transcripts relative to the controls, a significant trend was observed in the effect of triptolide on the nuclear, DVLA, and mitochondrial genes as shown in Figure 10. The nuclear genes, β-actin and EF1-α, were inhibited to a greater degree than all other genes tested. However, β-actin and EF1-α did not show a significant difference in inhibition from each other and. While DVLA loop was less inhibited, it was not significantly different from β-actin but was significantly different from EF1-α. The mitochondrial

genes were the least affected by the triptolide treatment and significantly less than the nuclear genes. DVLA stem was significantly less inhibited than the nuclear genes and slightly more inhibited than the mitochondrial genes. However, none of the DVLA or mitochondrial genes showed a statistical difference when compared with each other in response to triptolide inhibition. 89-734 was tested three separate times to test reproducibility and showed no statistical difference between the replicate experiments (data not shown). The healthy cultures also showed that the mitochondrial genes were inhibited less by Triptolide exposure than the nuclear genes, but it was not a significant difference.

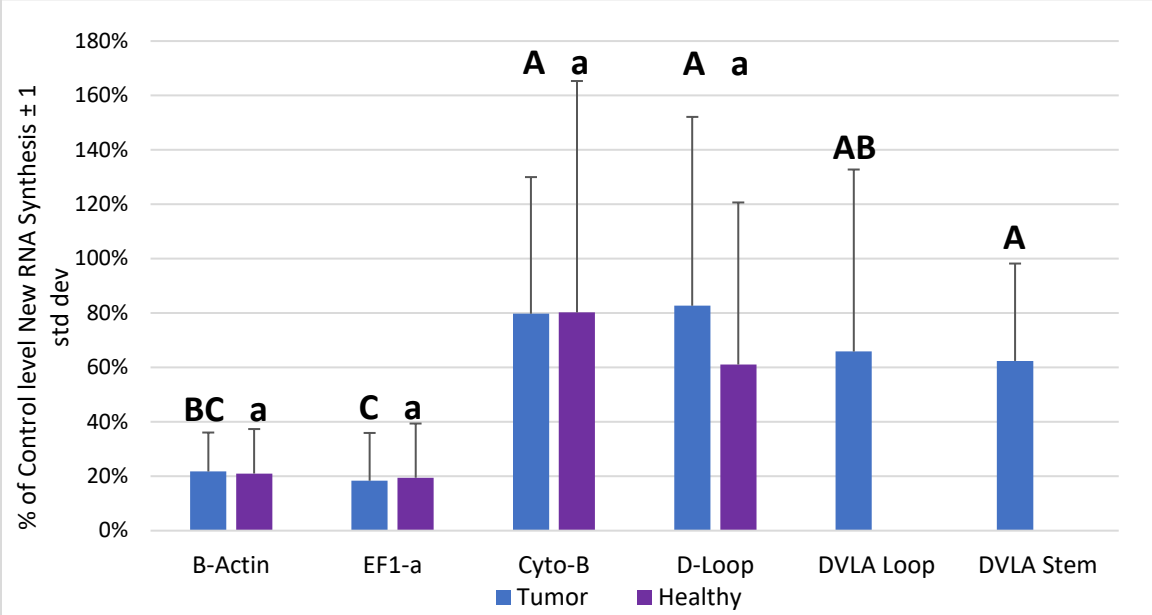

Figure 10: Change in new synthesis copy numbers between the controls and 0.1uM Triptolide samples. The change is plotted as a percentage and grouped as Tumor derived vs healthy cell lines. The letters above each gene shows which gene is significantly different from each other ($p<0.05$, Mann-Whitney U test). Same letters indicate no statistical difference. Upper case letters represent Tumor-derived cell lines and lower case letters represent healthy celll lines.

Mitochondrial RNA transcription inhibition with EtBr

Figure 11 shows the results from the inhibition of mitochondrial polymerase on 89-734 and 86-583 tumor cell lines treated with EtBr. The 50nM dose of EtBr was not

strong enough to cause an effect on transcription in these two cell lines and was dropped from subsequent analysis. The remaining dosages, 100 and 500nM, were pooled together and used for statistical analysis. New RNA synthesis was lower in the DVLA and mitochondrial genes than the nuclear genes. EF1-α was significantly less affected by treatment with EtBr than all other genes (Mann Whitney U test vs. cytochrome-b: $p< 0.01$, vs. D-loop: $p< 0.01$, vs. DVLA stem: $p< 0.01$, vs. β-actin: $p< 0.05$; vs. DVLA loop: $p< 0.05$). β-actin was also significantly less affected by EtBr when compared to both DVLA and mitochondrial genes. Both mitochondrial genes and both DVLA genes were significantly more affected by EtBr exposure than the nuclear genes. There were no statistical differences in the effect of EtBr on any of the DVLA or mitochondrial genes.

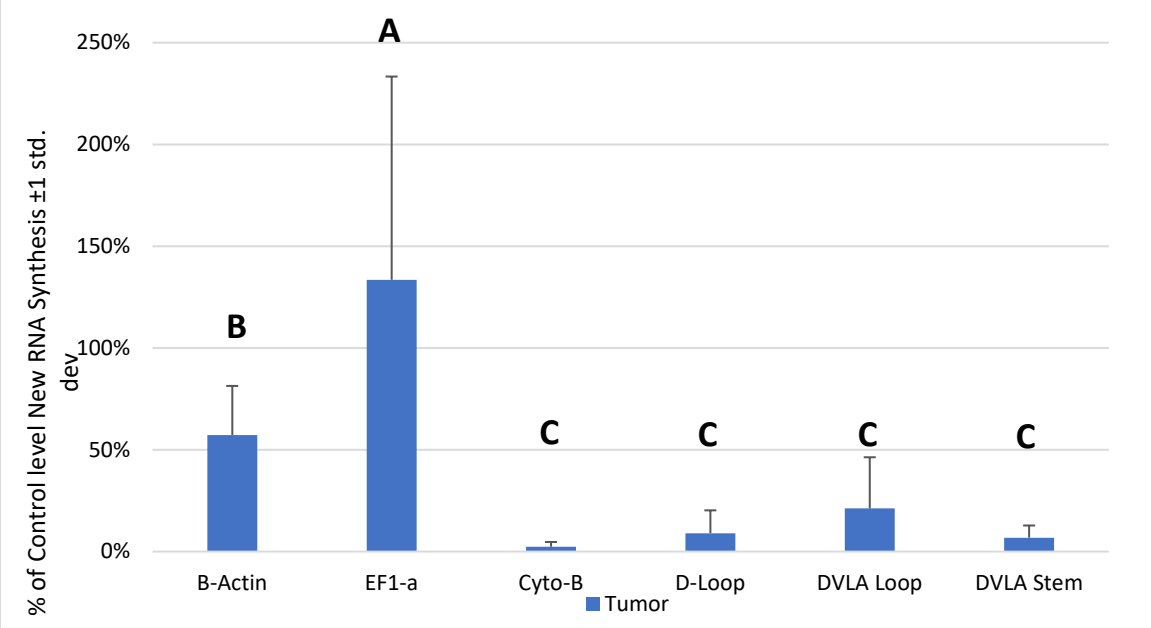

Figure 11: Change in new synthesis copy numbers between the controls and EtBr treatments. EtBr dosages are pooled together for analysis. The change is plotted as a percentage and 89-734 and 86-583 data are pooled. The letters above each gene shows which gene is significantly different from each other ($p<0.05$, Mann-Whitney U test). Same letters indicate no statistical difference.

Chapter 4- Discussion

Since DVLA may represent the only known infectious agent of mitochondria in animals, identifying the exact location and method of transcription is crucial to understanding the life cycle of this agent and the disease process. A critical component of this understanding is to determine the location of transcription of DVLA messages. Previous work has suggested it was located within the mitochondrial but was not confirmed.

Inhibition of RNA polymerase II Transcription with alpha-amanitin

Initial experiments were conducted to investigate how inhibition of RNA Polymerase II would affect DVLA transcription. If DVLA is being transcribed within the mitochondria as suspected then inhibition of RNA pol II should have a lesser effect on the DVLA or mitochondrial transcripts than the nuclear transcripts. These experiments showed variable results with both the DVLA and mitochondrial genes, particularly DVLA stem and cytochrome-b. This inconsistency could have been caused by trying to measure the change in total RNA concentrations. This method is not sensitive enough to allow for observation of an immediate transcription changes when RNA pol II is inhibited. Furthermore, alpha-amanitin undergoes a slow uptake process that spans several hours (6). Another issue with alpha-amanitin inhibition is that it is killing the cells by causing degradation of the RNA polymerase II by specifically targeting the Rpb1 subunit (6). This eventually causes reduced transcription for all the genes and makes finding differences even harder. To account for this in later experiments, RNA synthesis was measured through 4sU labeling. However, alpha-amanitin proved not to be the

correct drug of choice as it caused either no change in transcription or a complete shutdown of all genes thus providing a really small window for error. Treatment with alpha-amanitin can cause an accumulation of p53 within the cells. This could lead to the induction of apoptosis by activating p53 target genes (6). This could explain the results seen in the synthesis experiments as apoptosis would cause a decrease in the DVLA and mitochondrial transcripts and one cell line may be more susceptible to apoptosis than another.

4sU RNA Synthesis and Total RNA transcription levels

Initial experiments were conducted to test the effectiveness of the 4sU labeling method in fish cell culture. Cells were labeled for two and six hours to establish optimal labeling times (data not shown). Six hours provided the best measurement of new RNA transcription which usually ranged from one to five percent of the total RNA collected after the biotinylation and separation steps consistent with what was seen in previous works on this method which labelled murine fibroblasts for one hour with 200 μM 4sU at 37°C (31). The cultures used here were raised and maintained at 28°C which accounts for the slower incorporation seen in these experiments. Total RNA calculations were derived from all 6hr 4sU synthesis controls and used to establish relative levels of the transcripts across cell lines. They were also used to make comparisons about the abundance of the transcripts to each other and how they are correlated to each other. The two nuclear transcribed genes, β-actin and EF1-α, were the first and second most abundant transcripts for every cell line signifying their importance in the cells. This is similar to previous work that looked at the effectiveness of using different housekeeping genes in studying

the effect of estrogen in fish. EF1-α was found to be a highly expressed gene in liver and gonad tissues while β-actin showed low levels in liver tissue and high levels in gonad tissue (18). Other work in Atlantic salmon showed that β-actin varied considerably between different tissues while EF1-α remains stable between tissues except for in muscle tissues but they were both still two highly expressed genes (25). Following β-actin and EF1-α in abundance in the damselfish cell cultures were cytochrome-b and DVLA stem. New RNA synthesis of these two transcripts were also strongly correlated with each other and typically followed similar patterns in the inhibition experiments. DVLA loop and D-loop were found in the lowest abundance in the cells and were also strongly correlated to each other. The D-loop region of the mitochondria initiates transcription under the control of three mitochondrial promoters. D-loop RNA also serves as primer for mitochondrial DNA replication (4). Thus far no promoters have been found for DVLA but the DVLA loop RNA may serve as a primer for DVLA DNA replication. These data suggest that these two regions could serve a similar role of initiation of transcription. β-actin, EF1-α, and DVLA stem had lower synthesis in relation to the total RNA concentration compared to the other genes suggesting that they may have a longer turnover time in the cells while both mitochondrial genes and DVLA had higher synthesis. Furthermore, there are no statistical differences in these patterns between the tumor derived and healthy cell lines This would suggest that the presence of DVLA does not alter mitochondrial transcription. However, there were strong positive correlations in the new RNA synthesis between cytochrome-b, DVLA loop and DVLA stem as well as a strong positive correlation between D-loop and DVLA loop. This suggests that DVLA synthesis is facilitated by mitochondrial transcription. Nuclear and mitochondrial

transcription are linked together due to three mitochondrial transcription components being nuclear encoded including the mitochondrial RNA Polymerase (4). They also show a strong correlation in transcription based on the energy requirements of the different tissues. High energy demanding tissues will also undergo greater mitochondrial transcription (29). This could be beneficial for the DVLA genes because if they are responding to mitochondrial transcription then it would also lead to increased DVLA transcription in high energy tissues.

Estimated half-life calculations coincide with the RNA synthesis data wherein β-actin, EF1-α, and DVLA stem have longer half-life times to match their lower synthesis rates. This may relate to the class of genes these transcripts belong to. Different gene functions require longer half-lives as described by Friedel et al (19). Shorter half-lives are usually common for genes involved in transcription or signal transduction which coincides to the short half-life times seen for DVLA loop and D-loop. While longer half-lives are typically representative of genes used in metabolism and cell respiration (19). While these cell cultures used are maintained at 28°C rather than 37°C, the mitochondrial half-life results coincide with Piechota et al (30) that measured mitochondrial half-lives to be between one to seven hours. Another factor affecting RNA half-lives is the extent of poly-adenylation on the genes. As mentioned before, poly-adenylation is usually essential in stabilizing mRNA. Because DVLA transcripts are most likely not poly-adenylated they would be expected to be less stable (7, 9, 20, 30). This could probably be applied to DVLA loop but not DVLA stem as it has the longest half-life of all the genes tested including the nuclear transcribed genes. This would suggest that DVLA stem may

undergo another unique method for enhancing its stability compared to other non-polyadenylated mRNAs.

Inhibition of RNA polymerase II synthesis with Triptolide effects on DVLA

Further analysis of RNA Polymerase II inhibition was conducted by treating the cell lines with 0.1μM triptolide. Triptolide comes from a traditional Chinese medicinal plant and inhibits RNA polymerase II transcription in humans by binding to a subunit of the transcription factor TFIIH (43). Triptolide prevents the initiation of transcription by binding to the XPB subunit of TFIIH and preventing formation of the transcription bubble (6, 43). Triptolide was used to provide a better window of opportunity for measuring inhibition prior to complete cell shutdown unlike what was seen with alpha-amanitin previously because it has a faster uptake and different mode of inhibition. Inhibition with triptolide showed a decrease in RNA transcription across all genes tested. However, the nuclear genes showed significantly greater inhibition than either of the mitochondrial genes and DVLA stem. DVLA loop showed no significant difference from the nuclear genes nor the mitochondrial genes. DVLA also appears to be an intermediate of the nuclear genes and the mitochondrial genes as it seems to be affected slightly more than the mitochondrial genes. These results suggest that DVLA is not being transcribed by RNA pol II. The decrease across all genes could also be explained by the facts that ultimately the mitochondrial RNA polymerase is transcribed by the newly discovered SpRNAP-IV (28) and the three D-loop transcription factors are transcribed by RNA pol II (28) and thus their transcription could have been slowing down during the six-hour labeling time and lost.

Inhibition of mitochondrial RNA synthesis with EtBr effects on DVLA

Measuring mitochondrial inhibition is often difficult because it should be done in a way that it affects the mitochondria only. The mitochondria are also highly impermeable to most agents and must be made permeable for them to work which adds other confounding factors. Therefore, a lot of work has been done using isolated mitochondrial rather than intact cells. However, EtBr can penetrate mitochondria and decrease mitochondrial DNA replication and RNA transcription (14). The experiments here showed that the mitochondrial genes were significantly inhibited by the presence of EtBr. In addition, the DVLA transcripts were also significantly inhibited suggesting that they are transcribed by the same machinery as the mitochondrial genes. The nuclear genes show no appreciable inhibition in the presence of EtBr even at the highest concentration suggesting that EtBr is not affecting RNA pol II in any way. EtBr inhibits mitochondrial RNA transcription and DNA replication by binding to the mitochondrial DNA (14). This would cause a decrease in DVLA transcription as well because DVLA does not have its RNA polymerase and must rely on the host cell's machinery. Previous work already shows that DVLA DNA replicates within the mitochondria and the results seen here further suggest that DVLA RNA is also being transcribed in the mitochondria.

Conclusions

Inhibition with triptolide caused significantly less of an impact on DVLA transcription than on nuclear gene transcription suggesting that it is not connected to RNA polymerase II. Further evidence for this conclusion is shown by the EtBr data,

where DVLA and mitochondrial transcription were significantly inhibited while the nuclear genes were significantly less inhibited. In both inhibition experiments, DVLA behaved similarly to the mitochondrial RNAs. Based on the data presented here, DVLA transcription appears to be facilitated by the mitochondrial transcription machinery. Furthermore, the DVLA transcript levels showed strong positive correlations with the mitochondria genes and not the nuclear genes. The presence of DVLA also caused no significant effect on mitochondrial transcription or copy numbers. Therefore, DVLA does not appear to be inhibiting or enhancing mitochondrial transcription. DVLA loop may serve a similar function as D-loop in the initiation of transcription and as a primer for DVLA DNA replication. These two genes are strongly correlated to each other. During mitochondrial transcription, D-loop is part of a full-sized, heavy-strand pre-splice transcript that gives rise to smaller mitochondrial transcripts (1). DVLA loop may be serving a similar function and may be spliced to form the smaller transcripts recognized by the DVLA stem primer. Consistent with the pre-splice transcript hypothesis both D-loop and DVLA loop have short half-lives and high synthesis suggesting that they are more transient genes. During mitochondrial DNA replication, D-loop serves as a primer for heavy strand replication and DVLA may also be serving a similar function of DVLA DNA replication (1). DVLA stem has the longest half-life of all the genes tested with low synthesis rates suggesting that the stem transcripts undergo very little RNA degradation, thus causing it to be a longer lasting gene. This is inconsistent with the fact that DVLA stem is not poly-adenylated which means that it should be highly unstable. Therefore, DVLA stem RNA may have other unique properties that enhance stability.

Works Cited

1. Agaronyan, K., Morozov, Y. I., Anikin, M., & Temiakov, D. (2015). Replication-Transcription Switch in Human Mitochondria. *Research Reports, 347*(6221), 548-550.
2. Akins, R. A., Kelley, R. L., & Lambowitz, A. M. (1986). Mitochondrial Plasmids of Neurospora: Integration into Mitochondrial DNA and Evidence for Reverse Transcription in Mitochondria. *Cell, 47*, 505-516.
3. Arnold, J. J., Sharma, S. D., Feng, J. Y., Ray, A. S., Smidansky, E. D., Kireeva, M. L., . . . Cameron, C. E. (2012). Sensitivity of Mitochondrial Transcription and Resistance of RNA Polymerase II Dependent Nuclear Transcription to Antiviral Ribonucleosides. *PLOS Pathogens, 8*(11), 1-12.
4. Arnold, J. J., Smidansky, E. D., Moustafa, I. M., & Cameron, C. E. (2012). Human Mitochondrial RNA Polymerase: Structure-function, Mechanism, and Inhibition. *Biochimica et Biophysica Acta, 1819*(9-10), 948-960.
5. Baric, R. S., Nelson, G. W., Fleming, J. O., Deans, R. J., Keck, J. G., Casteel, N., & Stohlman, S. A. (1988). Interactions between Cornavirus Nucleocapsid Protein and Viral RNAs: Implications for Viral Transcription. *Journal of Virology, 62*(11), 4280-4287.
6. Bensaude, O. (2011). Inhibiting Eukaryotic Transcription. *Transcription, 2*(3), 103-108.
7. Borowski, L. S., Szczesny, R. J., Brzezniak, L. K., & Stepien, P. P. (2010). RNA Turnover in Human Mitochondria: More Questions than Answers? *Biochimica et Biophysica Acta, 1797*(6-7), 1066-1070.
8. Bralha, F. N., Liyanage, S. U., Hurren, R., Wang, X., Hi Son, M., Fung, T. A., . . . Laposa, R. R. (2015). Targeting Mitochondrial RNA Polymerase in Acute Myeloid Leukemia. *Oncotarget, Vol. 6, No. 35, 6*(35), 37216-37228.
9. Chang, J. H., & Tong, L. (2012). Mitochondrial Poly(A) Polymerase and Polyadenylation. *Biochimica et Biophysics Acta, 1819*(9-10), 992-997.
10. Chartier, A., Klein, P., Pierson, S., Barbezier, N., Gidaro, T., Casas, F., . . . Simonelig, M. (2015). Mitochondrial Dysfuntion Reveals the Role of mRNA Poly(A) Tail Regulation in Oculopharyngeal Muscular Dystrophy Pathogenesis. *PLOS Genetics, 11*(3), 1-27.
11. Chen, C.-Y. A., Ezzeddine, N., & Shyu, A.-B. (2008). Messenger RNA Half-Life Measurements in Mammalian Cells. *National Institute of Health, 448*, 335-357.

12. Claus, C., Manssen, L., Hubner, D., Robmark, S., Bothe, V., Petzold, A., . . . Liebert, U. G. (2015). Activation of the Mitochondrial Apoptotic Signaling Platform during Rubella Virus Infection. *Viruses, 7*, 6108-6126.

13. Coucheron, D. H., Nymark, M., Breines, R., Karlsen, B. O., Andreassen, M., Jorgensen, T. E., . . . Johansen, S. D. (2011). Characterization of Mitochondrial mRNAs in Codfish Reveals Unique Features Compared to Mammals. *Curr Genet, 57*, 213-222.

14. Desjardins, P., Frost, E., & Morais, R. (1985). Ethidium Bromide-Induced Loss of Mitochondrial DNA from Primary Chicken Embryo Fibroblasts. *Molecular and Cellular Biology, 5*(5), 1163-1169.

15. Dignam, J. D., Lebovitz, R. M., & Roeder, R. G. (1983). Accurate Transcription Initiation by RNA Polymerase II in a Soluble Extract from Isolated Mammalian Nuclei. *Nucleic Acids Research, 11*(5), 1475-1489.

16. Dolken, L., Ruzsics, Z., Radle, B., Friedel, C. C., Zimmer, R., Mages, J., . . . Koszinowski, U. H. (2008). High-resolution Gene Expression Profiling for Simultaneous Kinetic Parameter Analysis of RNA Synthesis and Decay. *RNA, 14*, 1959-1972.

17. Ferrer-Orta, C., Arias, A., Escarmis, C., & Verdaguer, N. (2006). A Comparison of Viral RNA-dependent RNA Polymerases. *Current Opinion in Structural Biology, 16*, 27-34.

18. Filby, A. L., & Tyler, C. R. (2007). Appropriate 'Housekeeping' Genes for Use in Expression Profiling the Effect of Environmental Estrogens in Fish. *BMC Molecular Biology, 8*(10).

19. Friedel, C. C., Dolken, L., Ruzsics, Z., Koszinowski, U. H., & Zimmer, R. (2009). Conserved Principles of Mammalian Transcriptional Regulation Revealed by RNA half-life. *Nucleic Acids Research, Vol. 37, No. 17, 37*(17), 1-12.

20. Gagliardi, D., Stepien, P. P., Temperley, R. J., Lightowlers, R. N., & Chrzanowska-Lightowlers, Z. M. (2004). Messenger RNA Stability in Mitochondria: Different Means to an End. *TRENDS in Genetics, 20*(6), 260-267.

21. Gaudray, G., Gachon, F., Basbous, J., BIard-Piechaczxk, M., Devaux, C., & Mesnard, J.-M. (2002). The Complementary Strand of the Human T-Cell Leukemia Virus Type 1 RNA Genome Encodes a bZIP Transcription Factor That Down- Regulates Viral Transcription. *Journal of Virology, 76*(24), 12813-12822.

22. Grant Jr., V. U., Moreno, S., Varela-Ramirez, A., & Johnson, K. L. (2014). Two Membrane-Associated Regions within the Nodamura Virus RNA-Dependent RNA Polymerase Are Critical for both Mitochondrial Localization and RNA Replication. *Journal of Virology, 88*(11), 5912-5926.

23. Hintz, W. E., Carneiro, J. S., Kassatenko, I., Varga, A., & James, D. (2013). Two Novel Mitoviruses from a Canadian Isolate of the Dutch Elm Pathogen Ophiostoma Novo-Ulmi (93-1224). *Virology Journal, 10*.

24. Hong, J.-R. (2013). Betanodavirus: Mitochondrial Disruption and Necrotic Cell Death. *World Journal of Virology, 2*(1), 1-5.

25. Ingerslev, H.-C., Pettersen, E. F., Jakobsen, R. A., Petersen, C. B., & Wergeland, H. I. (2006). Expression Profiling and Validation of Reference Gene Candidates in Immune Relevant Tissues and Cells from Atlantic Salmon (Salmo salar L.). *Molecular Immunology, 43*(8), 1194-1201.

26. Kao, C.-Y., & Read, L. K. (2005). Opposing Effects of Polyadenylation on the Stability of Edited and Unedited Mitochondrial RNAs in Trypanosoma brucei. *Molecular and Cellular Biology, 25*(5), 1634-1644.

27. Lai, M. M. (1998). Cellular Factors in the Transcription and Replication of Viral RNA Genomes: A Parallel to DNA-Dependent RNA Transcription. *Virology, 244*, 1-12.

28. Lee, Y.-L., Chiao, C.-H., & Hsu, M.-T. (2011). Transcription of Muscle Actin Genes by a Nuclear Form of Mitochondrial RNA Polymerase. *PLoS ONE 6(7), 6*(7), 1-8.

29. Mercer, T. R., Neph, S., Dinger, M. E., Crawford, J., Smith, M. A., Shearwood, A.-M. J., . . . Mattick, J. S. (2011). The Human Mitochondrial Transcriptome. *Cell, 146*, 645-658.

30. Piechota, J., Tomecki, R., Gewartowski, K., Szczesny, R., Domochowska, A., Kudla, M., . . . Bartnik, E. (2006). Differential Stability of Mitochondrial mRNA in HeLa Cells. *Acta Biochimica Polonica, 53*(1), 157-167.

31. Radle, B., Rutkowski, A. J., Ruzsics, Z., Friedel, C. C., Koszinowski, U. H., & Dolken, L. (2013). Metabolic Labeling of Newly Transcribed RNA for High Resolution Gene Expression Profiling of RNA Synthesis, Processing, and Decay in Cell Culture. *Journal of Visualized Experiments*(78).

32. Rahn, J. J., Gibbs, P. D., & Schmale, M. C. (2004). Patterns of Transcription of a Virus-like Agent in Tumor and Non Tumor Tissues in Bicolor Damselfish. *Comparative Biochemistry and Physiology, Part C, 138*(3), 401-409.

33. Rovnak, J., & Quackenbush, S. L. (2002). Walleye Dermal Sarcoma Virus Cyclin Interacts with Components of the Mediator Complex and the RNA Polymerase II Holoenzyme. *Journal of Virology, 76*(16), 8031-8039.

34. Rovnak, J., & Quackenbush, S. L. (2010). Walleye Dermal Sarcoma Virus: Molecular Biology and Oncogenesis. *Viruses, 2*, 1984-1999.

35. Saffran, H. A., Pare, J. M., Corcoran, J. A., Weller, S. K., & Smiley, J. R. (2007). Herpes Simplex Virus Eliminates Host Mitochondrial DNA. *European Molecular Biology Organization Reports, 8*(2), 188-193.

36. Schmale, M. (1991). Prevalence and Distribution Patterns of Tumors in Bicolor Damselfish (Pomacentrus partitus) on South Florida Reefs. *Marine Biology, 109*(2), 203-212.

37. Schmale, M. C. (1995). Experimental Induction of Neurofibromatosis in Bicolor Damselfish. *Disease of Aquatic Organisms, 23*, 201-212.

38. Schmale, M. C., Hensley, G. T., & Udey, L. R. (1986). Neurofibromatosis in the Bicolor Damselfish (Pomacentrus partitus) as a Model of von Recklinghausen Neurofibromatosis. *Annals New York Academy of Sciences, 486*, 386-402.

39. Schmale, M., Gibbs, P., & Campbell, C. (2002). A Virus-like Agent Associated with Neurofibromatosis in Damselfish. *Diseases of Aquatic Organisms, 49*(2), 107-115.

40. Sharova, L. V., Sharov, A. A., Nedorezov, T., Piao, Y., Shak, N., & Ko, M. S. (2009). Database for mRNA Half-Life of 19977 Genes Obtained by DNA Microarray Analysis of Pluripotent and Differentiationg Mouse Embryonic Stem Cells. *DNA Research, 16*(1), 45-58.

41. Shetty, M., Maiti, B., Santhosh, K. S., Venugopal, M. N., & Karunasagar, I. (2012). Betanodavirus of Marine and Freshwater Fish: Distribution, Genomic Organization, Diagnosis, and Control Measures. *Journal of Virology, 23*(2), 114-123.

42. Su, Y. C., Chiu, H. W., Hung, J. C., & Hong, J. R. (2014). Beta-nodavirus B2 Protein Induces Hydrogen Peroxide Production Leading to Drp1-recruited Mitochondrial Fragmentation and Cell Death via Mitochondrial Targeting. *Apoptosis, 19*, 1457-1470.

43. Titov, D. V., Gilman, B., He, Q.-L., Bhat, S., Low, W.-K., Dang, Y., . . . Liu, J. O. (2011). XPB , a Subunit of TFIIH , is a Target of the Natural Product Triptolide. *Nature Chemical Biology, 7*, 182-188.

44. Uddin, M. J., Suen, W. W., Prow, N. A., Hall, R. A., & Bielefeldt-Ohmann, H. (2015). West Nile Virus Challenge Alters the Transcription Profiles of Innate Immune Genes in Rabbit Peripheral Blood Mononuclear Cells. *Frontiers in Veterinary Science, 2*(76), 1-14.